

## Analysis of Discharge Sound and I-V Characteristic on Gliding Arc Discharge

**Streszczenie.** W celu analizy złożonego mechanizmu niehomogenicznego przestrzennie i czasowo wyładowania ze ślizgającym się łukiem przeanalizowano charakterystyki prądowo-napięciowe oraz dźwiękowe. Do celów badawczych zaproponowano nową metodę - mikrofon optyczny, który umożliwił obserwację fali ciśnieniowej powstałej po pojedynczym wyładowaniu w powietrzu. (Analiza charakterystyk prądowo-napięciowych i dźwiękowych w wyładowaniu ze ślizgającym się łukiem)

**Abstract.** Electrical and sound characteristics of gliding arc have been taken to analyze and discuss the discharge mechanism, which is very complex due to the plasma non-uniformity in space and time. New technique of optical wave microphone was introduced to observe generation of compressional wave after one pulsed discharge in air.

**Słowa kluczowe:** wyładowanie ze ślizgającym się łukiem, mikrofon optyczny

**Keywords:** gliding arc discharge, optical wave microphone

### Introduction

Plasma-chemical applications such as exhaust gas cleaning, disinfection or decontamination, organic compounds' decomposition and nanomaterials' production require high electron temperature and density but also low gas temperature [1-8]. However, conventional thermal plasma or non-thermal plasma generators can barely satisfy these conditions simultaneously. Gliding arc discharge allows on concurrent formation of both states of plasma: thermal and non-thermal one [9-17]. The gliding arc discharge starts from arc at the shortest gap between two divergent electrodes and it glides along gas flow. The arc cannot maintain when its length exceeds critical value and then transition from thermal to non-thermal plasma occurs. These processes are repeated periodically. This transitional discharge is very attractive but it is also non-uniform in time and space. Therefore, fundamental investigations, especially on frequency analysis of discharges and system optimization for electrode material, geometry of electrodes, frequency of power supply, breakdown ignition system, etc. are needed to make accurate control of the gliding arc discharge.

We have focused on compressional wave generated by electric discharge because it includes information about discharge current and atmospheric condition around discharge. A condenser microphone has been used to detect audible discharge sound wave, however it was impossible to set it in close position to the discharge electrodes where electric field was very strong. On the other hand, optical measurements such as beam deflection, Shadowgraph and Schlieren have been employed to avoid the complications caused by the additional noise. However, their sensitivity is relatively lower than that of a microphone, then it is recognized that they are useful especially to detect intense compressional wave like shock wave.

Here, we introduce a new optical method, named "an optical wave microphone" [18, 19], which is expected to substitute for conventional microphones or optical methods mentioned above. The optical wave microphone is a unique technique, which can detect compressional wave, change of density in gas medium, or even in liquid medium with a probe laser, a Fourier lens and a detector. Proposed technique is based on Fraunhofer diffraction between compressional wave and a probe laser and it is very useful to detect not only audible sound but also ultrasonic wave or shock wave without disturbing propagation of

compressional wave and electric field in the case of electric discharge.

Theoretical explanation of the optical wave microphone is as follows. When a probe laser beam crosses refractive index change such as sound wave at  $(x_0, y_0)$ , diffracted waves are generated and propagate with and in the penetrating beam through a Fourier optical lens to finally reach the detector. Detector should be placed within Fraunhofer diffraction region or in the back focal plane  $(x_f, y_f)$  of the Fourier lens. The diffracted optical wave is homodyne-detected by using the penetrating optical wave as a local oscillating power. The optical wave distribution  $u_w(x_f, y_f)$  at the detector position is shown in the next equation.

$$(1) \quad u_w(x_f, y_f) = \int_{-\infty}^{\infty} \int_{-\infty}^{\infty} u_w(x_0, y_0) T(x_0, y_0) \exp\{ik_i(x_0 x_f + y_0 y_f) / f\} dx_0 dy_0$$

here,

$u_w(x_0, y_0)$ :	complex amplitude of laser at $(x_0, y_0)$
$T(x_0, y_0)$ :	component of phase modulation by refractive index change
$k_i$ :	wave number of laser
$\lambda$ :	wave length of laser
$f$ :	focal length of Fourier lens

In this paper, frequency properties on discharge current and discharge sound waveforms of gliding arc discharge and their relationship were analyzed by FFT (Fast Fourier Transform). Measurements of propagating in air compressional wave, which is emitted by generation of plasma in gliding arc discharge were carried out with a conventional microphone and an optical wave microphone.

### Experimental setup

A schematic diagram of gliding arc discharge circuit with the evaluation equipment is shown in Fig. 1. Two divergent rod electrodes were made of iron ( $\phi=2$  mm, purity 99.5%). The divergent angle and length of the each electrode were  $20^\circ$  and 114 mm, respectively, and their shortest gap was 1 mm. Outlet ( $\phi=5$  mm) of a gas supply was placed 2 cm below the shortest gap. The gas flow rate was controlled by a digital flowmeter. High voltage (sine wave, 60 Hz) was applied between two electrodes via a high voltage transformer (VIC international, 120:1).

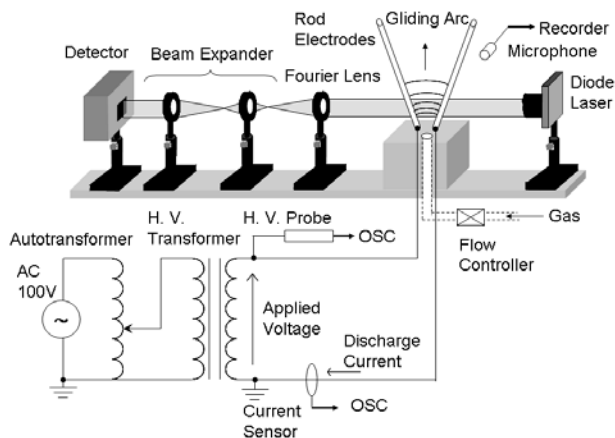


Fig. 1. Schematic diagram of gliding arc discharge circuit with evaluation equipment

The amplitude was adjusted with a voltage slide autotransformer (TAMABISHI, S-130-39). Applied voltage and current waveforms were observed during discharge with a high voltage probe (IWATSU, HV-P60) and by clamping a current sensor (HIOKI, 9018-50), respectively. Discharge sound was recorded with a microphone, which was set 50 cm apart from the electrodes. The optical wave microphone system, presented in Fig. 1. consisted of a diode laser, Fourier lens, a beam expander and the detector. The discharge electrodes were placed between the diode laser and the Fourier lens. The probe laser beam ( $w_0=2$  mm, 28 mW) was set 1 cm apart from the electrodes and at the same height as that of the shortest discharge gap in parallel to the discharge direction. Two lenses after the Fourier lens play a role of the beam expander. The diffraction signal, which was caused by interaction between the laser beam and the discharge sound wave was detected with the detector.

## Results and discussion

The consecutive experiments with changing of experimental parameters such as kinds of gas, gas flow rate, electrode material and geometry of electrode for a gliding arc discharge were carried out. We consider that influence of each parameter should be distinguished because it was found from the preliminary experiment that discharge phenomenon changes drastically with physical conditions.

In order to deepen the knowledge about fundamental characteristics of gliding arc discharge, part of the data was collected without flowing gas. Therefore, spatial position of arc discharges was almost fixed at around a shortest gap between electrodes. All measurements were carried out immediately after setting new iron electrodes since there was discharge time dependence on the degree of electrode's surface oxidation.

Figure 2(a) shows waveforms of applied voltage and current versus time during discharge. Figure 2(b) presents enlarged waveforms, which corresponds to the region described by the rectangular broken line in Fig. 2(a). As it can be seen in Fig. 2(a), two discharge current peaks were observed around maximum applied voltage, and four discharge current peaks occurred in one cycle of applied voltage. It should be noticed that a current peak consisted of a series of pulsed arc discharges, as shown in Fig. 2(b). Polarity dependence was confirmed and it was evident that intensity of positive discharge current peaks was higher than that of negative peaks by a factor of about four.

In Fig. 2(b) current after positive discharge, (possibly ion current), remained until generation of the next negative discharge. Thus, negative discharge current was lower than

that of positive discharge one because of the weakened effective electric field during the negative voltage application.

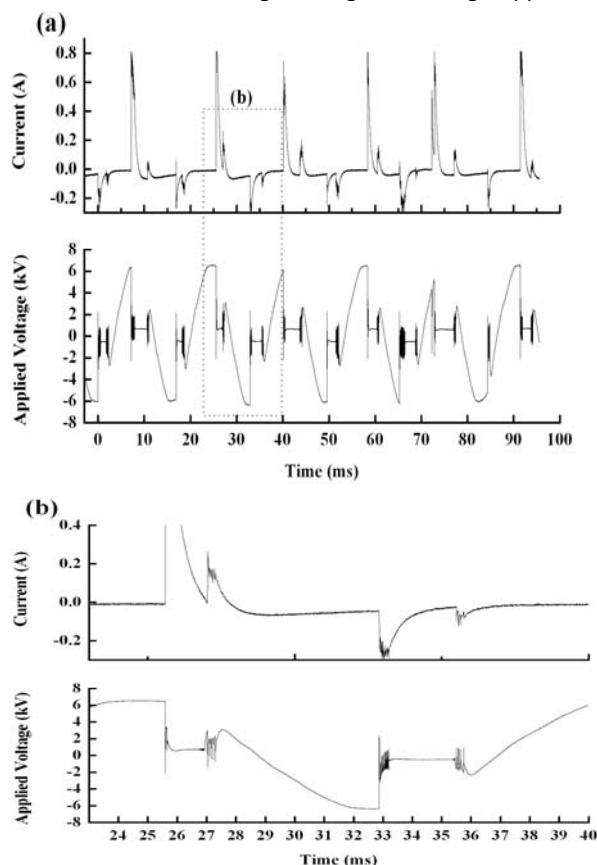


Fig. 2(a). Waveforms of applied voltage and current versus discharge time. (b) Enlarged waveforms, which correspond to the region described by the rectangular broken line in part (a)

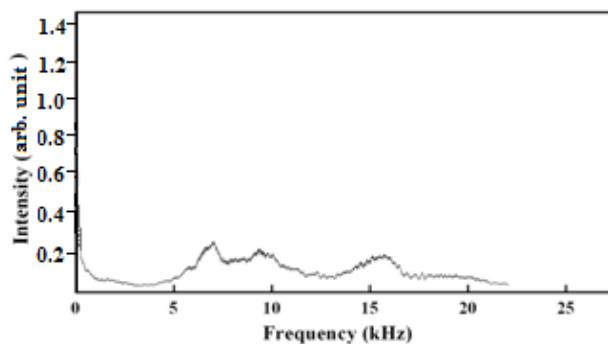


Fig. 3. FFT spectrum of the discharge sound recorded with a microphone

On the other hand, current after negative discharge attenuated completely, which means flow of space charge was finished and neutral state was recovered. This difference of current after positive and negative discharges resulted in strength of positive and negative discharges.

Figure 3 depicts a FFT spectrum for audible discharge sound, which was recorded with a microphone (sampling rate 44 kHz) set 50 cm apart from electrodes. Because it was impossible to set it close to electrodes, recorded sound waveform could not be synchronized with current waveform time delay due to sound velocity must be taken into account. The FFT spectrum was composed from mainly three peaks, which were relatively broad, approximately at 7 kHz, 9 kHz and 16 kHz.

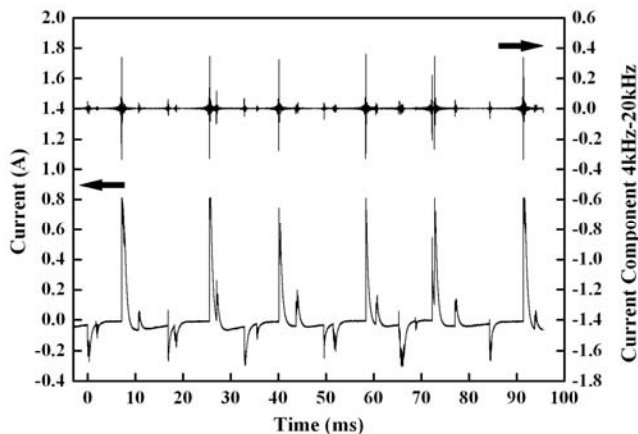


Fig. 4. FFT filtering result of the discharge current (4 kHz – 20 kHz)

Figure 4 is the FFT filtering result of the discharge current shown in Fig. 2(a). The current component from 4 kHz to 20 kHz was extracted to investigate correlation with the FFT of the audible discharge sound. There is a consistency of the current component (4 kHz to 20 kHz) with the series of the pulsed discharges that can be seen from the comparison between Fig. 2(b) and Fig. 4. These results indicated that frequency of pulsed discharges, especially, relatively intense discharges generated during positive applied voltage has correlation with audible discharge sound.

To analyze the relationship between continuity of pulsed discharges and audible sound, it was necessary to detect compressional wave after one pulsed discharge.

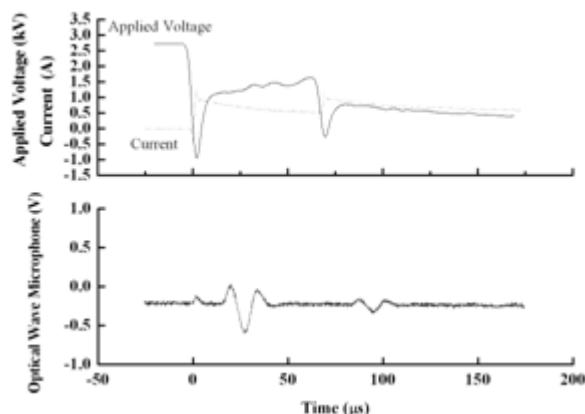


Fig. 5. The optical wave microphone measurement with corresponding waveforms of applied voltage and current

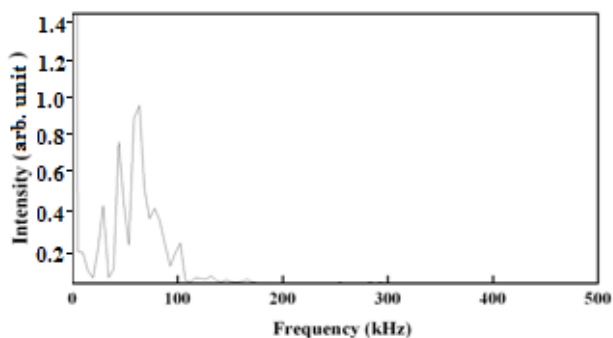


Fig. 6. FFT spectrum of the optical wave microphone signal

Figure 5 shows waveforms of applied voltage, current and optical wave microphone signal with shorter time scale. Two pulsed discharges were captured at 0  $\mu$ s and 70  $\mu$ s. It was estimated from widths of the voltage drop and the current pulse that one pulsed arc discharge continued for less than 10  $\mu$ s. A small signal, which appeared at 0  $\mu$ s in the optical wave microphone result was caused by an intense electromagnetic field generated due to strong arc current. Two compressional waves were observed in the optical wave microphone waveform just after the two pulsed arc discharges. The detection period was limited by the diameter of the probe laser beam.

Figure 6 is FFT spectrum of the optical wave microphone waveform. The range of the component was from several tens kHz to 100 kHz. No audible frequency was found. From the frequency of the signal and the time delay caused by sound velocity after discharge, it is suggested that the compressional wave in this case is ultrasonic wave because the frequency included higher component than audible sound and the velocity was almost the same as that of sound. The compressional wave generation after one pulsed discharge was detected experimentally. It was confirmed that each compressional wave was the origin of the audible sound detected with the microphone. Detail measurements to confirm possibility of accurate shock wave generation by pulsed arc discharge are necessary.

## Conclusions

Analysis of discharge current and sound were carried out by introducing a new compressional wave detection system based on an optical wave microphone. The results were summarized as follows:

- 1) Mainly two discharge current peaks appeared at maximum applied voltage.
- 2) The current peak consisted of a series of pulsed discharges.
- 3) Remarkably high polarity dependence of the discharge current was observed. Positive discharge current was larger compared to that of negative discharge.
- 4) Frequency components of audible discharge sound corresponded to the frequency of the pulsed discharges.
- 5) Generation of compressional wave after one pulsed discharge was detected with the optical wave microphone technique.

## Authors:

Prof. dr. Fumiaki Mitsugi, E-mail: mitsugi@cs.kumamoto-u.ac.jp, Prof. dr. Tomoaki Ikegami, Graduate School of Science and Technology, Kumamoto University, Kurokami 2-39-1, Kumamoto 860-8555, Japan; Prof. dr. Shin-ichi Aoki, Department of Computer and Information Science, Sojo University, Ikeda 4-22-1, Kumamoto 860-0082, Japan; Prof. dr. Toshiyuki Nakamiya, Prof. dr. Yoshito Sonoda, Graduate School of Industrial Engineering, Tokai University, 9-1-1 Toroku, Kumamoto 862-8652, Japan; Prof. dr. Hiroharu Kawasaki, Department of Electrical and Electronics Engineering, Sasebo National College of Technology, 1-1 Okisin, Sasebo 857-8171, Japan; D. Sci. Joanna Pawlat, E-mail: askmik@hotmail.com, Prof. D. Sci. Henryka Stryczewska, Institute of Electrical Engineering and Electrotechnologies, Lublin University of Technology, 38A Nadbystrzycka St., 20-618 Lublin, Poland.

## REFERENCES

- [1] Stryczewska H., Pawlat J., Ebihara K, Non-thermal plasma aided soil decontamination JAOTs, (2013), 1(16): 23-30
- [2] Ebihara K., Mitsugi F., Ikegami T., Nakamura N., Hashimoto Y., Yamashita Y. Baba S., Stryczewska H., Pawlat J., Teii S., Sung T., Ozone-mist spray sterilization for pest control in agricultural management EPJAP, (2013), 61(02): 201324318
- [3] Hensel K., Kučerová K., Tarabová B., Janda M., Machala Z., Sano K., Mihai C., Gorgan L., Jijie R., Pohoata V., Topala I.,

- Effects of air transient spark discharge and helium plasma jet on water, bacteria, cells and biomolecules, *Biointerphases* (2015), 10(2): 029515
- [4] Pawłat J., Atmospheric pressure plasma jet for decontamination purposes, *EPJAP* (2013), 61(2): 201324323
- [5] Fojtikova P., Radkova L., Janova D., Krcma F., Application of Low-temperature Low-pressure Hydrogen Plasma: Treatment of Artificially Prepared Corrosion Layers, *Open Chemistry* (2015), 13(1): 362-368
- [6] Pawłat J., Samoń R., Stryczewska H., Diatczyk J., Giżewski T. RF-powered atmospheric pressure plasma jet for surface treatment, *EPJAP*, (2013), 61(2): 201324322,
- [7] Dors M., Nowakowska H., Jasiński M., Mizeraczyk J., Chemical Kinetics of Methane Pyrolysis in Microwave Plasma at Atmospheric Pressure, *Plasma Chemistry and Plasma Processing*, (2014), 34(2):313-326
- [8] Kocik M., Dors M., Podlinski J., Mizeraczyk J., Kanazawa S., Ichiki R., Sato T., Characterisation of pulsed discharge in water, *EPJAP*, (2013), 64: 10801
- [9] Diatczyk J., Modeling discharge length for GA plasma reactor, *Przeгляд Elektrotechniczny*, (2012), 6(88): 89-91
- [10] Stryczewska H., Jakubowski T., Kalisiak S., Giżewski T., Pawłat J., Power systems of plasma reactors for non-thermal plasma generation<sup>9</sup>, *JAOTs*, (2013), 16(1): 52-62
- [11] Pawłat J., Diatczyk J., Stryczewska H., Low-temperature plasma for exhaust gas purification from paint shop - a case study, *Przeгляд Elektrotechniczny*, (2011), 1: 245-248
- [12] Schmidt-Szalowski K., Krawczyk K., Młotek M., Catalytic Effects of Metals on the Conversion of Methane in Gliding Discharges, *Plasma Processes and Polymers* (2007), 7-8: 728-736
- [13] Diatczyk J., Jaroszyński L., Komarzyniec G., Stryczewska H. D., Modelowanie reaktorów ze ślizgającym się wyładowaniem łukowym, *Technologie Nadprzewodnikowe i Plazmowe w Energetyce*, Lubelskie Towarzystwo Naukowe, Lublin, 2009, 207-239
- [14] Stryczewska H., Wac-Włodarczyk A., Goleman R., Nalewaj K., Giżewski T., Jaroszyński L., Komarzyniec G., Mazurek P., Diatczyk J., Urządzenia elektrotechnologiczne stosowane w energetyce i ekologii, *Przeгляд Elektrotechniczny*, (2013), 5: 346-352
- [15] Raniszewski G., Temperature measurements in arc-discharge synthesis of nanomaterials dedicated for medical applications, *EPJAP*, (2013), 61(2): 24311
- [16] Stryczewska H., Diatczyk J., Pawłat J., Temperature Distribution in the Gliding Arc Discharge Chamber, *JAOTs* (2011), 2(14): 276-281
- [17] Mitsugi F., Ohshima T., Kawasaki H., Kawasaki T., Aouki S., Baba T., Kinouchi S., Gas flow dependence on dynamic behavior of serpentine plasma in gliding arc discharge system, *IEEE Transactions on Plasma Science*, (2014), 42(12): 3681-3686
- [18] Sonoda Y., Ochi S., Matsuo K., Muraoka K., Akazaki M., Evans D., Measurements of plasma-waves by the Fraunhofer-diffraction method at two-point intersections, *JJAP* (1984), 23: 1412-1413
- [19] Mitsugi F., Ikegami T., Nakamiya T., Sonoda Y., Observation of Phenomena After Pulsed Laser Irradiation of Solid with Optical Wave Microphone, *JJAP* 51(1S): 01AC10